https://doi.org/10.15407/ujpe70.3.170

G.M. CARMEL VIGILA BAI,[1] R. ABISHA[2,3]

[1] Assistant Professor, Department of Physics, Government Arts and Science College
(Konam, Nagercoil-629 004, Tamilnadu, India; e-mail: gmcarmelvb@gmail.com)
[2] Department of Physics, Rani Anna Government College For Women
(Tirunelveli-08 Tamilnadu, India; Reg. No. 19221172132007; e-mail: abisharusselraj@gmail.com)
[3] Affiliated to Manonmaniam Sundaranar University, Abhishekapatti
(Tirunelveli-12, Tamilnadu, India)

THEORETICAL CALCULATION OF TWO-PROTON DECAY HALF LIVES USING THE HULTHEN POTENTIAL IN A MODIFIED CYE MODEL

Using a MCYE (modified Cubic plus Yukawa plus Exponential) model, we will thoroughly examine the two-proton radioactivity half-lives [1]. Additionally, we employ this model to forecast the half-lives of various two-proton emitters. Our anticipated outcomes are in line with those attained from other pertinent models. The model is improved by including the total diproton-daughter nucleus interaction potential Hulthen-type electrostatic term in the two-sphere approximation, as well as by examining the effects of this in the half-life time values. The computed 2*p radioactive half-lives are discovered to be in excellent accord with the other theoretical model predictions, such as CPPMDN model of K.P. Santhosh, the GLDM, ELDM, GLM, SEB, and UFM models.*

K e y w o r d s: 2*p*- radioactivity, Hulthen potential, half-live.

1. Introduction

The simultaneous release of two protons from a nuclear ground state, that is, close to or over the proton drip line, each having a measurable half-life, is known as the two-proton radioactivity. Proton pairing may participate in the 2*p* radioactivity phenomena, when the nuclei with an even proton number (even $-Z$) are situated in proximity to the proton drip line. 2 proton (2*p*) radioactivity have been 1st discovered by Zel'dovich in the 1960s [2], and Goldansky later went on to explain the system [3]. The diproton correlations for the 2*p* decay of ^{12}O were conducted in 1978. The nuclear binding energy led to the conclusion that it was a diproton emitter. For a very long period, study on the ^{16}Ne isotope according to the nuclear binding energy, It was believed to be an emitter of diproton [4]. In a vicinity of the proton drip line, the first experimental attempts to access isotopes of light 2*p* unbound nuclei were made in 1984 [5]. In 1991, two protons might be regarded as a single quasi-particle called a "diproton" with a charge of two and a mass of two [6]. In 1996 the 2*p* decay of the activated ^{14}O nucleus caused by the reaction of resonance $^{13}\mathrm{N}+\mathrm{P}$ [7] was studied. In ^{17}Ne, the first excited state 3/2 is a fascinating 2*p* decay candidate. Numerous experimental attempts to investigate this state have been made [8]. A brand-new technique for analysing 2*p* decay was developed by Mukha *et al.* in 2001. It is ideal for the in-flight analysis of very short-lived 2*p* emitters and complements implantation operations in gases and solids [9]. The first genuine 2*p* emitter was finally discovered in the decay of ^{45}Fe in 2002, after more than 40 years of research [10, 11]. In addition, the GANIL group found ^{54}Zn [12], another 2*p*-emitting isotope Mukha *et al.* [13] found another fascinating example of 2*p* radioactivity in 2006 from the high-lying 21+ isomer in ^{94}Ag. Ra-

Citation: Carmel Vigila Bai G.M., Abisha R. Theoretical calculation of two-proton decay half lives using the Hulthen potential in a modified CYE model. *Ukr. J. Phys.* **70**, No. 3, 170 (2025). https://doi.org/10.15407/ujpe70.3.170.

dioactivity involving two protons is handled as 2-body problem, where a cluster of decaying valance protons occurs. Consequently, asymptotic behavior of 3 bodies is broken, and a significant amount of the specific information regarding the valence proton configurations is lost. This study was done in 2006 by Rotureau *et al.* [14] utilizing the continuum's embedded shell model framework. The ground-breaking research utilized to investigate the two-proton radioactivity of ^{19}Mg was revealed in 2007 [15]. Using silicon microstrip detectors, the in-flight decay approach painstakingly reconstructs the routes of all decay products. Direct observation of $2p$ radioactivity and research into the p–p correlation (TPC) were made possible in 2007 and 2008 employing time-projection chambers that are gaseous. The proton track projections on the TPC's anode plane can be recorded thanks to these detectors, verifying the $2p$ emission from the ^{45}Fe decay [16]. A brand-new optical TPC detector (OTPC) was subsequently used to photograph each unique $2p$ decay event of ^{45}Fe [17]. Mukha *et al.* conducted research on the ^{16}Ne isotope in 2008 using the recently developed in-flight decay technology [18]. In 2009, Grigorenko [19] examined the radioactivity of two protons as a 3-body (core $+p$ p) problem using the harmonics that are hyper spherical approach. Anther proton emitter, ^{8}C, should also be recognized for the year 2010. It was once believed that the simultaneous emission of 4 protons would cause this isotope to decay. The $2p$ decay of the ^{12}O [20] and ^{16}Ne [21] was experimentally investigated using the invariant mass technique. The 4^{th} $2p$ emitter, ^{67}Kr with a half-life of a few milliseconds, was eventually found in 2016 at the fragment separator Big RIPS in RIKEN by a French team. [22]. In 2019 [23], a new $2p$-unbound isotope, ^{11}O, was found. In a pilot study in 2019, the novel $2p$-emitting isotopes ^{29,30}Ar and the FRS will be put to the test. Numerous publications using different theoretical frameworks have been written by several authors and characterize $2p$ radioactivity as a ^{2}He cluster decay process. Effective liquid drop model (ELDM) [24], empirical formulas [25], GLDM (generalised liquid drop model) [26], GLM (Gamow like model) [27], CPPMDN (Coulomb & proximity potential model for deformed nuclei) [28], and New Geiger–Nuttall Law [29] are some of the theoretical models that have been utilized since 2006 to analyze $2p$ radioactivity and its half-lives. Additionally, these methods have been successfully applied to several real sources to duplicate the experimental $2p$ radioactive half-lives.

The features of α decay, cluster decay, as well as Fission degradation that occurs spontaneously of actinide, transactinide, and extremely heavy nuclei with and without incorporate deformation effects were investigated in our previous works using the CYE model [30–35]. To thoroughly explore the half-lives of $2p$ radioactivity, the Cubic Plus Yukawa exponential model (CYE) was modified for this work, and utilized to investigate the emission of 2 protons from a variety of proton-rich nuclei. We have figured out the half-life of $2p$ decay for various emitters [36–39]. In the current work, we have added the Hulthen potential to the CYEM calculation of the two-proton decay half-lifetimes.

2. CYE (Cubic Plus Yukawa Plus Exponential) Model

In current investigation, We have employed a practical framework [40], recognized as the CYE model to investigate the characteristics of deterioration. As, the zero-point Energy from vibration is specifically mentioned. At a certain distance from the nucleus, the proton pairs are already there, and the proton particle only comes into contact with pure Coulomb potential. For the post-splitter region, this potential is given by a function of r, the separation among the mass centers of the 2 parts,

$$V(r) = \frac{Z_1 Z_2 e^2}{r} + V_n(r) - Q; \quad r \geq r_t, \tag{1}$$

where $V_n(r)$ is expressed as the nuclear interaction energy in the form

$$V_n(r) = -D\left[F + \frac{r - r_t}{a}\right]\frac{r_t}{r}\exp\left[\frac{r_t - r}{a}\right].$$

Here, r_a and r_b are the integrand's 2 suitable zeros.

3. Opportunities for the Region after Scission

The parent along with daughter nuclei are regarded as spherical in this work. The potential for the post-scission is provided by, if the ejected nucleus is spherical, the daughter nucleus only shows one deformation, like a quadrupole deformation, and, if the origin of the reaction is taken to be its Q value, shown below

$$V(r) = V_c(r) + V_n(r) - V_{df}(r) - Q; \quad r \geq r_t, \tag{2}$$

$V_c(r)$ is the Coulomb potential among the fragment that is released and the spheroidal daughter, V_n(r) is limited range effects on the nuclear interaction energy, V_{df}(r) is a change in the energy of nuclear interaction brought on by the daughter nucleus' quadrupole deformation ($\beta 2$).

It will be taken into account that a prolate spheroid daughter nucleus possesses a larger axis in the fission plane

$$V_c\left(r\right)=\frac{3}{2}\frac{Z_1Z_2e^2\gamma}{r}\left[\frac{1-\gamma^2}{2}\ln\frac{\gamma+1}{\gamma-1}+\gamma\right]. \tag{3}$$

In the case of an oblate spheroid daughter, the shorter axis is in the fission direction

$$V_c\left(r\right)=\frac{3}{2}\frac{Z_1Z_2e^2}{r}\left[\gamma\left(1+\gamma^2\right)\arctan\gamma^{-1}-\gamma^2\right]. \tag{4}$$

Here

$$\gamma=\frac{r}{\left(a_2^2-b_2^2\right)^{1/2}}.$$

The radius vector $R(\theta)$ that locates the sharp nucleus surface that has been distorted, when the nuclei are spheroid-shaped, the information at an angle θ in relation to the symmetry axis is given by

$$R\left(\theta\right)=R_0\left[1+\sum_{n=0}^{\infty}\sum_{m=-n}^{n}\beta_{nm}Y_{nm}(\theta)\right]. \tag{5}$$

Here, R_0 is the corresponding radius of a spherical nucleus.

The variation in the energy of nuclear interactions resulting from the daughter nucleus' quadrupole deformation $\beta 2$ can be found by

$$V_d=\frac{4R_2^3C_sA_2\beta_2}{ar_0^2}\left(\frac{5}{4\pi}\right)^{1/2}.$$

4. The PRE-Scission Area

A 3-order polynomial in r approximates the barrier's shape that has a potential in the overlaid area between the "ground state, as well as the meeting point. We have

$$V(r)=-E_v+\left[V(r_t)+E_v\right]\left\{s_1\left[\frac{r-r_i}{r_t-r_i}\right]^2-\right.$$
$$\left.-s_2\left[\frac{r-r_i}{r_t-r_i}\right]^3\right\};\quad r_i\le r\le r_t. \tag{6}$$

That is, $rt=a2+R1$, and ri is the distance among the center of mass of two daughter sections and the released nuclei in the spheroidal parent nucleus. Here, depending on the shape, $a2$ is either the semimajor or minor axis of the spheroidal daughter nucleus.

With regard for the spheroid deformation $\beta 2$,

$$R\left(\theta\right)=R_0\left[1+\beta_2\left(\frac{5}{4\pi}\right)^{1/2}\left(\frac{3}{2}\cos^2\theta-\frac{1}{2}\right)\right] \tag{7}$$

and deformation may additionally include the Nilsson's hexadecapole deformation $\beta 4$. Then Eq. (5) becomes

$$R(\theta)=R_0\left[1+\beta_2\left(\frac{5}{4\pi}\right)^{1/2}\left(\frac{3}{2}\cos^2\theta-\frac{1}{2}\right)+\right.$$
$$\left.+\beta_4\left(\frac{9}{4\pi}\right)^{1/2}\frac{1}{8}\left(35\,\cos^4\theta-30\,\cos^2\theta+3\right)\right]. \tag{8}$$

The system's half-life is estimated using the relation:

$$T=\frac{1.433\times10^{-21}}{E_v}\left[1+\exp(K)\right], \tag{9}$$

where

$$K=\frac{2}{\hbar}\int_{r_a}^{r_t}\left[2B_r\left(r\right)V(r)\right]^{1/2}dr+$$
$$+\frac{2}{\hbar}\int_{r_t}^{r_b}\left[2B_r\left(r\right)V(r)\right]^{1/2}dr.$$

For calculating the 0 point vibration energy E_v,

$$E_v=\frac{\pi\hbar}{2}\left[\frac{\left(\frac{2Q}{\mu}\right)^{1/2}}{(C_1+C_2)}\right],$$

C_1 and C_2 are the central radii of the fragments assigned by $C_i=1.18\,A^{1/3}-0.48$ $(i=1,2)$ and reduced mass,

$$\mu=\frac{m_1m_2}{m_1+m_2}.$$

5. Hulthen Potential Incorporation in Half-Life Time Calculation

We alter the CYE model by including the Hulthen potential $V_{\rm H}(r)$, an electrostatic potential of the exponential kind. The Hulthen potential is considered to

be the Coulomb potential. In the domains of atomic, solid state physics, along with molecular, this potential is used. IT exhibits the same behavior as the $V_C(r)$ at short distances ($r \to 0$) and declines exponentially more quickly over large distances ($r \gg 0$).

We have

$$V_H r = \frac{aZ_{2p}Z_d e^2}{e^{ar-1}}, \tag{10}$$

where a is the screening parameter, which might decide the potential's range, or the reduction of the escape radius.

6. Result and Discussion

In the current work, we have used the CYE model to perform assessments of the two-proton ($2p$) radioactive half-lifetimes for different emitters. Here, we have calculated the $2p$ radioactivity in the two-sphere approximation using the CYE model, modified CYE in the two-sphere approximation, and by using the Hulthen potential in MCYEM. Subsequently, we examined the deformation effects in $2p$ radioactivity only in MCYE model. First and second columns of Table 1 should list the nuclei with $2p$ radioactivity, the experimental Q_{2p} values, and We compare the half-life time values of our CYE model with other models without accounting for deformation effects, MGLM [29], and SEB [41] with experimental values (columns 3–7). Only in MCYE model, by including the hexacontatetrapole ($\beta 6$) deformation in the parent nucleus together with the quadrupole $\beta 2$ and hexadecaple $\beta 4$ deformations, we have attempted to analyze the two-proton decay features of elements with atomic numbers in the interval $Z = 16$–80 and are listed in Table 2. The potential barrier's height and width are reduced, when three-grid deformations are included. It is clear that this results in a large drop in the half lives of two-proton decay. The concepts of the deformation parameters are derived from Reference [42]. Our estimated half-lives, based on the computations, accord well with the other available data. Therefore, the nuclei's stability is improved by the hexacontatetrapole deformation ($\beta 6$). Figures 2 and 3 predict about the contour plot of half-life time values with and without deformation effects.

The screening parameter, $a = 1.436 \times 10^{-3}$ fm^{-1} in order to observe the way the $2p$-radioactive nucleus's charge Z and released energy Q_{2p} affect the electrostatic shielding effect. The value of the parameter determined by fitting the data from experimental values. The contour plot of half-life time values that incorporates the Hulthen potential is shown in

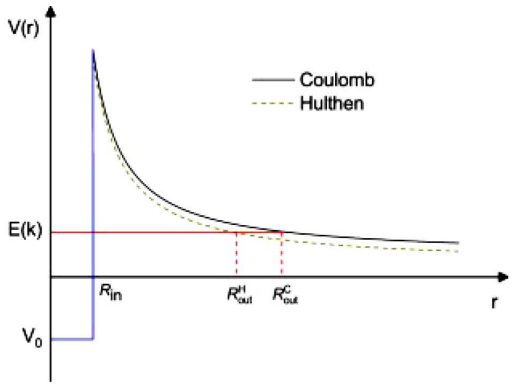

Fig. 1. Illustrates the relationship between the decay system's centre of mass and the Hulthen potential between the two protons that are released and the daughter nucleus

Table 1. **Calculated the $2p$ radioactivity in the two-sphere approximation using the CYE model, modified CYE in the two-sphere approximation, and by using the Hulthen potential in MCYEM**

Parent nuclei	Q_{2P} (MeV)	$\mathrm{Log}_{10}\, T_{1/2}(s)$				
		CYEM calculated	CYE model with Hulthen	Exp. values	MGLM [29]	SEB [40]
^{6}Be	1.372 [43]	–21.41	–21.42	$-20.30^{+0.03}_{-0.03}$ [43]	–	–19.86
^{12}O	1.638 [20]	–15.81	–15.83	>20.20 [20]	–	–17.70
^{16}Ne	1.401 [44]	–14.47	–14.49	$-20.38^{+0.03}_{-0.03}$ [44]	–	–15.71
^{19}Mg	0.750 [15]	–10.25	–10.29	$-11.40^{+0.14}_{-0.20}$ [15]	–11.39	–10.58
^{45}Fe	1.100 [10]	–1.94	–2.01	$-2.40^{+0.26}_{-0.26}$ [10]	–2.28	–2.32
^{48}Ni	1.290 [45]	–1.67	–1.73	$-2.52^{+0.24}_{-0.22}$ [45]	–2.69	–2.55
^{54}Zn	1.280 [46]	–0.9	–0.95	$-2.76^{+0.15}_{-0.14}$ [46]	–1.12	–1.31
^{67}Kr	1.690 [22]	0.11	0.04	$-1.70^{+0.02}_{-0.02}$ [22]	–0.84	–0.95

Table 2. **Comparison between the predicted half-lives for $2p$ from various nuclei by using MCYE model with three grid deformations (β_{2P}, β_{2D}, β_{4P}, β_{6P})**

Nuclei	Q_{2P} (MeV)	$\mathrm{Log}_{10}\, T_{1/2}(s)$			
		Without deformation		With deformation	CPPMDN [47]
		CYEM calculated	CYE model with Hulthen	CYE model with deformation β_{2P}, β_{4P}, β_{6P}, β_{2D})	
^{26}S	2.36	–16.43	–13.55	–18.29	–16.19
^{28}Cl	2.72	–13.65	–13.69	–12.30	–16.35
^{29}Ar	5.90	–18.51	–15.87	–18.08	–
^{30}Ar	3.42	–16.82	–14.18	–16.33	–17.35
^{32}K	2.74	–13.05	–13.09	–13.11	–15.61
^{33}Ca	5.13	–17.34	–14.39	–17.40	–
^{34}Ca	2.51	–12.18	–12.22	–13.49	–14.65
^{35}Sc	4.98	–14.16	–14.21	–15.22	–17.36
^{37}Sc	0.38	6.92	6.85	7.97	9.72
^{39}V	4.21	–15.65	–13.71	–13.72	–16.74
^{41}Cr	3.33	–12.17	–12.23	–12.72	–14.87
^{42}Cr	1.48	–5.67	–5.73	–5.35	–7.60
^{43}Mn	2.48	–10.14	–10.20	–10.53	–11.91
^{44}Mn	0.50	8.79	8.70	8.29	9.19
^{47}Co	1.02	0.94	0.85	1.13	0.11
^{49}Ni	1.08	0.92	0.83	0.50	–0.59
^{52}Cu	1.13	1.09	0.93	1.00	1.54
^{55}Zn	0.78	8.29	8.19	8.20	7.71
^{56} Ga	2.82	–8.18	–8.72	–8.27	–11.03
^{57}Ga	1.65	–2.16	–2.37	–2.24	–3.73
^{58}Ga	0.51	17.09	17.34	16.99	18.27
^{58}Ge	3.23	–9.47	–10.88	–9.55	–12.00
^{59}Ge	1.60	–1.29	–1.37	–2.10	–3.23
^{60}Ge	0.631	12.24	12.02	12.16	14.00
^{60}As	3.32	–9.45	–10.04	–9.51	–9.83
^{61}As	1.98	–3.19	–2.55	–3.28	–5.55
^{62}As	0.59	15.72	15.61	15.66	17.51
^{63}Se	2.36	–5.33	–6.51	–5.42	–7.26
^{64}Se	0.70	12.90	12.37	12.81	14.15
^{65}Br	2.43	–5.15	–5.10	–5.24	–6.42
^{66}Br	1.39	2.69	1.97	2.60	1.36
^{68}Kr	1.46	2.52	1.74	2.48	1.34
^{81}Mo	0.73	21.80	21.58	21.76	22.98
^{84}Ru	0.60	28.87	30.55	30.67	–
^{85}Ru	1.13	13.84	13.14	13.73	13.67
^{105}Te	0.24	27.95	23.36	24.62	–
^{108}Xe	1.01	24.68	24.28	24.52	26.64
^{120}Nd	0.33	74.17	73.23	76.35	–
^{126}Sm	0.24	100.89	100.15	103.22	–
^{150}Hf	1.16	35.74	37.69	33.10	–
^{154}W	1.25	24.74	24.08	24.29	–
^{159}Os	0.79	55.39	55.13	57.25	–
^{165}Pt	1.44	32.28	31.43	33.96	–
^{170}Hg	1.85	23.60	23.41	25.21	–

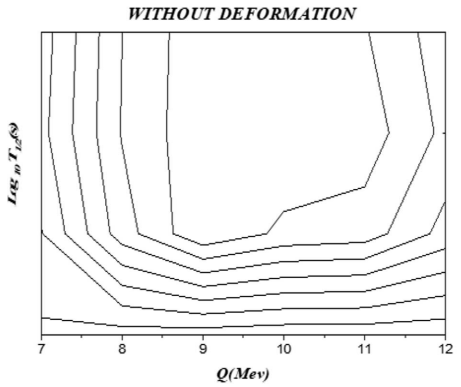

Fig. 2. Shows the contour plot of half-life time Fig. 3 shows the contour plot of half-life without including deformation values

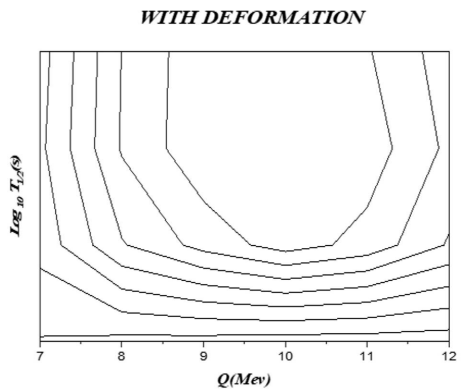

Fig. 3. Shows the contour plot of half-life time Fig. 3 shows the contour plot of half-life time values with including deformation values

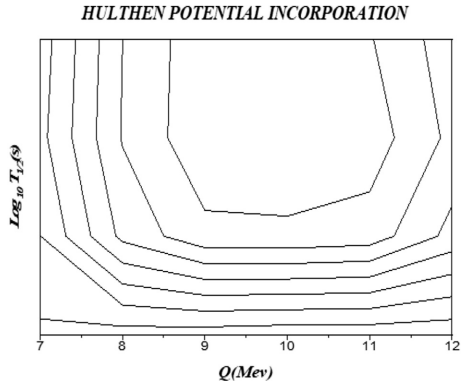

Fig. 4. Shows the contour plot of half-life time values with including Hulthen potential in the two-sphere approximation

Fig. 4. When compared to the contour plot of other graphs, the number of contours and the area of the inner closed contour are drastically reduced here. Accordingly, the addition of the Hulthen potential will result in a rise in the nucleus' half-life value.

7. Summary and Conclusion

In this study, the CYE model is used to determine the $2p$-decay half-life. The experimental and theoretical estimate of the $2p$-decay half time correspond perfectly. Comparing the contour plot of with adding deformation, to the contour plot of half-life time values including the Hulthen potential, the number of contours, as well as the area of inner closed contour, are greatly reduced. That demonstrates the enhanced stability of proton-rich nuclei. The calculated results within the CYEM model are in good agreement with the experimental data and other theoretical models. It may provide a theoretical reference for the future experiments.

1. G.M. Carmel Vigila Bai, R. Abisha. Possible $2p$ decay emission in the region $4 \leq Z \leq 54$ using modified CYE model. *Ukr. j. Phys.* **69** (3), 149 (2024).
2. Y.B. Zel'dovich. The existence of new isotopes of light nuclei the equation of state of neutrons. *Sov. Phys. JETP* **11**, 812 (1960).
3. V.I. Goldansky. On neutron-deficient isotopes of light nuclei and the phenomena of proton and two proton radioactivity. *Nucl. Phys.* **19**, 482 (1960).
4. G.J. KeKelis, M.S. Zisman, D.K. Scott, R. Jahn, D.J. Vieira, Joseph Cerny, F. Ajzenberg-Selove. Masses of the unbound nuclei ^{16}Ne, ^{15}F and ^{12}O. *Phys. Rev. C* **17**, 1929 (1978).
5. O.V. Bochkarev, A.A. Korsheninnikov, E.A. Kuz'min, I.G. Mukha, A.A. Ogloblin, L.V. Chulkov, G.B. Yan'kov. Two-proton decay of ^{6}Be. *JETP Letters* **40**, 969 (1984).
6. B. Alex Brown. Diproton decay of nuclei on the proton drip line. *Phys. Rev. C* **43**, R1513(R) (1991).
7. C.R. Bain, P.J. Woods, R. Coszach, T. Davinson, P. Decrock, M. Gaelens, W. Galster, M. Huyse, R.J. Irvine, P. Leleux, E. Lienard, M. Loiselet, C. Michotte, R. Neal, A. Ninane, G. Ryckewaert *et.al.* Two proton emission induced via a resonance reaction. *Phys. Lett. B* **373**, 35 (1996).
8. M.J. Chromik, B.A. Brown, M. Fauerbach, T. Glasmacher, R. Ibbotson, H. Scheit, M. Thoennessen, P.G. Thirolf. Excitation and decay of the first excited state of ^{17}Ne. *Phys. Rev. C* **55**, 1676 (1997).
9. I. Mukha, G. Schrieder. Two-proton radioactivity as a genuine three-body decay: The ^{19}Mg probe. *Nucl. Phys A* **690**, 280 (2001).
10. M. Pfützner, E. Badura, C. Bingham, B. Blank, M. Chartier, H. Geissel, J. Giovinazzo, L.V. Grigorenko, R. Grzywacz, M. Hellström. First evidence for the two-proton decay of ^{45}Fe. *Eur. Phys. J. A* **14**, 279 (2002).

11. J. Giovinazzo, B. Blank, M. Chartier, S. Czajkowski, A. Fleury, M.J. Lopez Jimenez, M.S. Praviko, J.C. Thomas, F. de Oliveira Santos, M. Lewitowicz, V. Maslov, M. Stanoiu, R. Grzywacz, M. Pftzner, *et. al.* Two-proton radioactivity of ^{45}Fe. *Phys. Rev. Lett.* **89**, 102501 (2002).
12. B. Blank *et al.* First observation of ^{54}Zn and its decay by two-proton emission. *Phys. Rev. Lett.* **94**, 232501 (2005).
13. I. Mukha, Ernst Roeckl, Leonid Batist, Andrey Blazhev, Joachim Doring, Hubert Grawe, Leonid Grigorenko, Mark Huyse, Zenon Janas, Reinhard Kirchner, Marco La Commara, Chiara Mazzocchi, Sam L. Tabor, Piet Van Duppen. Proton-proton correletions observed in two proton radioactivity of ^{94}Ag. *Nature* **439**, 298 (2006).
14. J. Rotureau, J. Okołowicz, M. Płoszajczak. Theory of the two-proton radioactivity in the continuum shell model. *Nucl. Phys. A* **767**, 13 (2006).
15. I. Mukha, K. Sümmerer, L. Acosta, M.A.G. Alvarez, E. Casarejos, A. Chatillon, D. Cortina-Gil, J. Espino, A. Fomichev, J.E. García-Ramos, H. Geissel, J. Gómez-Camacho, L. Grigorenko, J. Hoffmann, O. Kiselev, *et al.* Observation of two- proton radioactivity of ^{19}Mg by tracking the decay products. *Phys. Rev. Lett.* **99**, 182501 (2007).
16. J. Giovinazzo *et al.* First direct observation of two protons in the decay of ^{45}Fe with a time-projection chamber. *Phys. Rev. Lett.* **99**, 102501 (2007).
17. K. Miernik *et al.* Studies of charged particle emission in the decay of ^{45}Fe. *Acta Physica Polonica B* **39**, 477 (2008).
18. I. Mukha, L. Grigorenko, K. Sümmerer, L. Acosta, M.A.G. Alvarez, E. Casarejos, A. Chatillon, D. Cortina-Gil, J.M. Espino, A. Fomichev, J.E. García-Ramos, H. Geissel, J. Gómez-Camacho, J. Hofmann, O. Kiselev *et al.* Proton-proton correlations observed in two-proton decay of ^{19}Mg and ^{16}Ne. *Phys. Rev. C* **77**, 061303(R) (2008).
19. L.V. Grigorenko. Theoretical study of two-proton radioactivity. Status, predictions, and applications. *Phys. Part. Nucl.* **40**, 674 (2009).
20. M.F. Jager, R.J. Charity, J.M. Elson, J. Manfredi, M.H. Mahzoon, L.G. Sobotka, M. McCleskey, R.G. Pizzone, B.T. Roeder, A. Spiridon, E. Simmons, L. Trache, M. Kurokawa. Two-proton decay of ^{12}O and its isobaric analog state in ^{12}N. *Phys. Rev. C* **86**, 011304 (2012).
21. K.W. Brown, R.J. Charity, L.G. Sobotka, Z. Chajecki, L.V. Grigorenko, I.A. Egorova, Yu.L. Parfenova, M.V. Zhukov, S. Bedoor, W.W. Buhro, J.M. Elson, W.G. Lynch, J. Manfredi, D.G. McNeel, W. Reviol *et al.* Observation of longrange three-body coulomb effects in the decay of ^{16}Ne. *Phys. Rev. Lett.* **113**, 232501 (2014).
22. T. Goigoux, P. Ascher, B. Blank, M. Gerbaux, J. Giovinazzo, S. Grévy, T. Kurtukian Nieto, C. Magron, P. Doornenbal, G.G. Kiss, S. Nishimura, P.A. Söderström, V.H. Phong, J. Wu, D.S. Ahn *et al.* Two-proton radioactivity of ^{67}Kr. *Phys. Rev. Lett.* **117**, 162501 (2016).
23. T.B. Webb *et al.* First observation of unbound ^{11}O, the mirror of the halo nucleus ^{11}Li. *Phys. Rev. Lett.* **122**, 122501 (2019).
24. M. Gonalves, N. Teruya, O.A.P. Tavares, S.B. Duarte. Two proton emission half-lives in the effective liquid drop model. *Phys. Lett. B* **774**, 14 (2017).
25. I. Sreeja, M. Balasubramaniam. An empirical formula for the half-lives of exotic two-proton emission. *Eur. Phys. J. A* **55** 33 (2019).
26. J.P. Cui, Y.H. Gao, Y.Z. Wang, J.Z. Gu. Two proton radioactivity within a generalized liquid drop model. *Phys. Rev. C* **101**, 014301 (2020).
27. H.M. Liu, Y.T. Zou, X. Pan, You-Tian Zou, Jiu-Long Chen, Jun-Hao Cheng, Biao He, Xiao-Hua Li. Systematic study of two-proton radioactivity within a Gamow like model. *Chin. Phys. C* **45**, 044110 (2021).
28. K.P. Santhosh. Theoretical studies on two-proton radioactivity. *Phys. Rev. C* **104**, 064613 (2021).
29. H. M. Liu, Y.T. Zou, X. Pan De-Xing Zhu, Yang-Yang Xu, Xi-Jun Wu, Peng-Cheng Chu, Xiao-Hua Li. New Geiger Nuttall law for two-proton radioactivity. *Chin. Phys. C* **45**, 024108 (2021).
30. G. Shanmugam, B. Kamalaharan. Exotic decay model and alpha decay studies. *Phys. Rev. C* **41**, 1742 (1990).
31. G. Shanmugam, G.M. Carmel Vigila Bai, B. Kamalaharan. Cluster radiactivities from an island of cluster emitters. *Phys. Rev. C* **51**, 2616 (1995).
32. G.M. Carmel Vigila Bai, R. Nithya Agnes. Role of multi polarity-six deformation parameter on exotic decay half-life of Berkelium nucleus. *IOSR-Journal of Appl. Phys.* **3**, (2017).
33. G.M. Carmel Vigila Bai, J. UmaiParvathiy. Alpha decay properties of heavy and superheavy elements Pramana. *J. Physics* **84** (1), 113 (2015).
34. J. Umai Parvathy. *Properties of Superheavy Elements in Trans-Actinide Region.* Dr. Sci., Thesis (Manonmanium sundaranar university, 2016) (in Tirunelveli).
35. G.M. Carmel Vigila Bai, R. Revathi. Competition between alpha decay, cluster decay and spontaneous fission in the superheavy nuclei, $Z = 126$. *Math. Sci. Int. Res. J.* **7**, (2018).
36. G.M. Carmel Vigila Bai, R. Abisha. Two proton radioactivity of nuclei – $Z \geq 4$ to $Z \leq 36$. In: Proceedings of the International Conference of IVCARTMSN, May 24 (2022).
37. G.M. Carmel Vigila Bai, R. Abisha. Two proton Radioactivity of nuclei – $Z \geq 4$ to $Z \leq 54$. In: *Proceedings of the National Seminar on Functional Materials and Its Application NSFMA October 14* (2022) [ISBN: 978-93-84737-37-5].
38. G.M. Carmel Vigila Bai, R. Abisha. Two proton radioactivity of heavy and super heavy mass region – $Z \geq 100$ to $Z \leq 111$. In: *Proceedings of the International Conference on Interdisciplinary Research in Chemistry ICIRC'23, February 24–25* (2023) [ISBN: 978-93-5812-971-7].
39. G.M. Carmel Vigila Bai, R. Abisha. Two proton Radioactivity half-life time study using CYE model. In: *Proceedings of the DAE Symposium on Nuclear Physics* (2023) [ISBN: 978-81-959225-12].

40. G.M. Carmel Vigila Bai. *A Systematic Study of Cluster Radioactivity in Trans-Tin Region.* Dr. Sci., Thesis (Manonmanium Sundaranar University 1997) (in Tirunelveli).
41. You-Tian Zou, Xiao Pan, Xiao-Hua Li, Hong-Ming Liu, Xi-Jun Wu, Biao He. Systematic study of two-proton radioactivity with a screened electrostatic barrier. *Chin. Phys. C* **45**, 104102 (2021).
42. P. Möller, A.J. Sierk, T. Ichikawa, H. Sagawa. Nuclear ground state masses and deformations. *At. Data Nucl. Data Tables I* **109**, 1 (2016).
43. W. Whaling. Magnetic analysis of the Li^6(He^3, t) Be^6 reaction. *Phys. Rev.* **150**, 836 (1966).
44. C.J. Woodward, R.E. Tribble, D.M. Tanner. Mass of ^{16}Ne. *Phys. Rev. C* **27**, 27 (1983).
45. M. Pomorski, M. Pfützner, W. Dominik, R. Grzywacz, A. Stolz, T. Baumann, J.S. Berryman, H. Czyrkowski, R. Dabrowski, A. Fijalkowska, T. Ginter, J. Johnson, G. Kaminski, N. Larson, S.N. Liddick *et al.* Proton spectroscopy of ^{48}Ni, ^{46}Fe, ^{44}Cr. *Phys. Rev. C* **90**, 014311 (2014).
46. P. Ascher, L. Audirac, N. Adimi, B. Blank, C. Borcea, B.A. Brown, I. Companis, F. Delalee, C.E. Demonchy, F. de Oliveira Santos, J. Giovinazzo, S. Grevy, L.V. Grigorenko, T. Kurtukian-Nieto, S. Leblanc *et al. Phys. Rev. Lett.* **107**, 102502 (2011).
47. K.P. Santhosh. Two-proton radioactivity within a coulomb and proximity potential model for deformed nuclei. *Phys. Rev. C* **106**, 054604 (2022).

Received 21.03.24

Г.М.К.В. Бай, Р. Абіша

ТЕОРЕТИЧНИЙ РОЗРАХУНОК ЧАСІВ НАПІВРОЗПАДУ З ЕМІСІЄЮ ДВОХ ПРОТОНІВ В МОДИФІКОВАНІЙ CYE МОДЕЛІ З ПОТЕНЦІАЛОМ ХЮЛЬТЕНА

Досліджуються теоретично часи напіврозпаду з емісією двох протонів у MCYE моделі [1]. Враховується взаємодія двох протонів з дочірнім ядром. Результати добре узгоджуються з отриманими в інших моделях.

Ключові слова: 2*p*-радіоактивність, потенціал Хюльтена, час напіврозпаду.